LAWRENCE
LIVERMORE
NATIONAL
LABORATORY

LLNL-JRNL-402949

Surface chemistry driven actuation in nanoporous gold

J. Biener , A. Wittstock, L. Zepeda-Ruiz, M. M. Biener, V. Zielasek , D. Kramer, R. N. Viswanath, J. Weissmuller, M. Baumer, A. V. Hamza

April 15, 2008

Nature Materials

Disclaimer

Surface chemistry driven actuation in nanoporous gold

J. Biener,[1*] A. Wittstock,[1,2] L. Zepeda-Ruiz,[1] M. M. Biener, V. Zielasek,[2] D. Kramer,[3] R. N. Viswanath,[3] J. Weissmüller,[3] M. Bäumer,[2] A. V. Hamza[1]

[1] Nanoscale Synthesis and Characterization Laboratory, Lawrence Livermore National Laboratory, Livermore, USA
[2] Institut für Angewandte und Physikalische Chemie, Universität Bremen, Bremen, Germany
[3] Institut für Nanotechnologie, Forschungszentrum Karlsruhe, Karlsruhe, Germany

[*] To whom correspondence should be addressed. E-mail: biener2@llnl.gov

Although actuation in biological systems is exclusively powered by chemical energy, this concept has not been realized in man-made actuator technologies, as these rely on generating heat or electricity first. Here, we demonstrate that surface-chemistry driven actuation can be realized in high surface area materials such as nanoporous gold. For example, we achieve reversible strain amplitudes in the order of a few tenths of a percent by alternating exposure of nanoporous Au to ozone and carbon monoxide. The effect can be explained by adsorbate-induced changes of the surface stress, and can be used to convert chemical energy directly into a mechanical response thus opening the door to surface-chemistry driven actuator and sensor technologies.

In the most general definition, an actuator is a device which converts some sort of energy into mechanical work. Exploring nanostructured high-surface-area materials for this purpose has recently attracted much interest (*1-3*). Although the majority of the work in this field is focused on polymer and carbon nanotube based materials (*4*), macroscopic and reversible strain effects have also been observed for nanoporous metals in an electrochemical environment (*3, 5*). In particular nanoporous Pt and Au have been demonstrated to yield strain amplitudes comparable to those of commercial ferroelectric ceramics(*3, 5*). Although the microscopic processes behind the charge-strain response of nanoporous metals in an electrochemical environment are still under debate, it seems to be clear – in a continuum description – that the effect is caused by charge-induced changes in the surface stress *f* at the metal-electrolyte interface (*6*).

In the present report we describe an actuator concept which is based on *surface-chemistry induced* changes of the surface stress at a *metal-gas* interface which, in turn, drives an elastic macroscopic sample contraction/expansion. This concept can be used to directly convert chemical energy into a mechanical response *without* generating heat or electricity first. The underlying principle, adsorbate-induced changes of the surface stress *f* of metal surfaces, has been the subject of intensive research (*7, 8*). Covalent adsorbate-metal interactions seem to play a decisive role in determining both size and even sign of adsorbate-induced changes of *f* (*9*). Although the relative change in *f* can be large, a macroscopic strain response can only be achieved by using high-surface-area materials. In the following, we report on in-situ strain measurements on nanoporous gold. By using

the oxidation of carbon monoxide by ozone, $CO + O_3 \rightarrow CO_2 + O_2$, as a driving reaction we achieved reversible, macroscopic stains of up to 0.5%. Nanoporous Au is an ideal material for this experiment for several reasons: First and foremost, np- Au exhibits unexpected catalytic properties. The material is reactive enough to catalyze surface reactions such as ozone dissociation (*10*) and CO oxidation (*11*) at room temperature, but it is also noble enough to prevent irreversible oxidation. Second, its characteristic sponge-like open-cell foam morphology (*12*) makes it a high surface area material which also combines high porosity (mass transport) with high strength (sustainable stress) (*13*). Finally, ozone exposure can be expected to change the surface stress of Au as oxygen adsorption has been shown to cause a depletion of the Au 5d band (*14*).

Nanoporous Au can be easily prepared in the form of mm-sized monolithic samples by a process called 'dealloying'. In metallurgy, dealloying is defined as selective corrosion (removal) of the less noble constituent (here: Ag) from an alloy (Ag-Au), usually via dissolving this component in a corrosive environment (*12, 15*). In the case of Ag-Au alloys, this leads to the development of a three-dimensional bicontinuous nanoporous structure while maintaining the original shape of the alloy sample (see Figure 1). The test specimen used in the present work were prepared by dealloying 1 mm^3 cubes of a $Ag_{75}Au_{25}$ master alloy in standard three-electrode electrochemical setup using a one molar perchloric acid electrolyte (*16*). The resulting Au foam samples had a porosity of ~70%, and exhibit a specific surface area of ~10-15 m^2/g and a pore size of 10-20 nm. The strain measurements were performed in a commercial dilatometer equipped with a sealed sample compartment for environmental control.

Typical macroscopic strain versus time data sets are shown in Figure 2. Here the strain was continuously monitored while the samples were alternately exposed to a mixture of 1-8% O_3 in O_2 and pure CO. Splitting the surface catalyzed oxidation of CO by O_3 into two self-limiting half-reactions allows one to switch the surface of np-Au back and forth between an oxygen-covered and clean state: In the first half cycle, ozone exposure leads to oxygen adsorption on the clean Au surface (*17*), $O_3 + Au \rightarrow Au\text{-}O + O_2$, while CO exposure in the second half cycle restores the clean Au surface by reacting with adsorbed oxygen towards carbon dioxide (*11*), $CO + Au\text{-}O \rightarrow CO_2 + Au$. In contrast to oxygen, CO does not form a stable adsorbate layer on Au surfaces at room temperature, and the CO coverage will rapidly approach zero once the CO exposure is interrupted (*18*). The data shown in Fig. 2a reveal that O_3 exposure (chemisorption of oxygen) causes a sample contraction, while CO exposure restores the original sample dimensions by reacting with adsorbed oxygen (*19*). The strain amplitude increases with both cycle length (Fig 2c) and the O_3 concentration (Fig 2d), and typical strain values lie in the range from 0.05 to 0.5%. Note that a strain amplitude of 0.5 % corresponds to a macroscopic actuator stroke of 5 μm for a one-mm-long sample. A small irreversible component is superimposed on the elastic response, which becomes more pronounced for larger actuator strains. This might indicate plastic yielding or, more consistent with the slow kinetics, stress-driven diffusion creep.

Although we record only the uniaxial strain response $\Delta l/l$ of our system, it is truly a 3D phenomenon where in the limit of small strains the volume change $\Delta V/V$ is given by 3

$\Delta l/l$. Since np-Au can sustain macroscopic stresses of up to 200 MPa (*20*), the actuator concept described here has a *P*d*V* work density of ~3 MJ/m^3 which is comparable to that of a shape memory alloy based system described recently by Ebron et al. (*2*). The advantage of the surface-stress driven actuator concept described here is that maintaining the strain does not require the continuous supply of chemical energy. The efficiency of the actuator can be estimated from the standard Gibbs energy of reaction of the CO oxidation by O_3 (~420 kJ/mol), and the number of surface atoms (~1000 mol/m^3 for np-Au with a specific surface area of ~10 m^2/g and density of 6 10^6 g/m^3). Assuming a oxygen saturation coverage of approximately one (*21*) reveals an efficiency in the order of 1%. The low efficiency is a direct consequence of the strongly exothermic nature of our driving reaction. In principle, it should be possible to increase the efficiency by selecting reactions which are accompanied by small entropy and enthalpy changes. Note that the one-mm-cube samples used in the current study contain only ~10^{-6} mol of surface atoms thus making it a potentially very sensitive sensor material. For example, a miniaturized 10-micron cube could still produce an easy to detect 50-nm stroke which would translate in a detection limit as low as 10^{-12} mol.

The surface stress changes necessary to explain the observed macroscopic dimensional changes can be analyzed within a continuum approach. The starting point for such an analysis is the generalized capillary equation for solids (*22*) which relates the volumetric average of the pressure in the solid to the area average of the surface stress. Assuming that the measured dimensional change $\Delta l/l_o$ is the direct consequence of a surface-stress induced, linear elastic and isotropic lattice strain, one can show that the mean change of surface stress $<\Delta f>$ is related to $\Delta l/l_o$ via (*6, 23*)

$$\Delta f = -\frac{9K}{2\alpha_m \rho}\frac{\Delta l}{l_o} \qquad (1)$$

where K is the bulk modulus of the solid (220 GPa for Au), α_m is the specific surface area (10-15 m^2/g), and ρ is the bulk density (19.3 x 10^6 g/m^3 for Au). According to Eq. 1, a Δf of 17-26 N/m would be required to explain a compressive strain of 0.005. Although adsorbate-induced changes of f of up to 15 N/m have been reported for the Cs/Ni(111) system (*8*), the predicted surface stress change does appear unexpectedly high for oxygen adsorption. In fact, one of the assumptions involved in the derivation of Eq. (1) must be considered as a poor approximation for nanoporous gold, and the prediction for Δf must thus be viewed as qualitative here. The derivation rests on the assumption that the relative macroscopic volume change of the sample agrees with the volume change of the solid phase, which can be rigorously related to the surface stress change. This is valid when the deformation throughout the porous network can be approximated as an affine stretch. The assumption is plausible for compacts of approximately spherical powder particles of similar size, where it has indeed been confirmed by in-situ x-ray experiments (*3*). By contrast, the surface-induced stress in elongated objects - such as the ligaments in np-Au - will typically exhibit a significant shear component (*22*). The resulting strain will be nonuniform and locally anisotropic. A continuum mechanics analysis indicates that Eq. (1) may then overestimate the magnitude of Δf by (in extreme cases) as much as one order of magnitude, in particular for materials with a large Poisson number such as Au (*24*). In the absence of a 'calibration' the above results for Δf are therefore qualitative.

Molecular dynamics (MD) simulations offer just such an opportunity to independently test the surface stress-strain response of np-Au. Here, we performed fully atomistic MD simulations on the effect of surface stress on the equilibrium shape of realistic models of np-Au and its structural building blocks, the ligaments. The embedded atom method (EAM) potential used in this work generates a tensile surface stress of ~1.3 N/m (at 0 K) for the Au(100) surface in good agreement with the literature (*25*). The skeletal network of our computational np-Au samples was generated by simulating the spinodal decomposition during vapor quenching, and freezing the process once the desired length scale was achieved (*26*). The final structure was obtained by adjusting the ligament diameter to produce the desired porosity (~70%), and filling the ligament volume with Au atoms. (100)-oriented Au nanowires were used as models for the ligaments (Fig. 3a). Both samples were created using the atomic positions of bulk fcc Au. The effect of tensile surface stress was studied by equilibrating the samples to zero overall pressure at various temperatures ranging from 0 K to 300 K. The dimensional changes observed during this relaxation are caused solely by tensile surface stress, and therefore provide a benchmark for the thermodynamic surface stress – strain correlation. An inspection of figure 3b reveals that Eq.1 indeed underestimates the effect of surface stress: In the case of nanowires, the effect of tensile surface stress is an almost uniaxial contraction along the wire axis ($\Delta L/L \sim \Delta V/V$) and the contraction is approximately seven times larger than predicted by Eq. 1. The nanoporous samples, on the other hand, show isotropic contraction ($\Delta L/L \sim 1/3\ \Delta V/V$), and the relaxation is weaker, but still three times stronger than predicted by the thermodynamic approach. The differences between nanowires and np Au is consistent with the random network structure of the latter, and their lower surface-to-volume ratio. Besides the presence of local shear deformation, the stronger-than-predicted MD strain response may also reflect the extremely high fraction of step edge and kink site atoms (coordination number 7 and 6, respectively) of these samples. In view of the MD results, the experimentally observed strain levels of up to 0.005 can be explained by surface stress changes of ~6 N/m instead of the ~20 N/m predicted by the thermodynamic approach.

So far, we have only discussed the size of the adsorbate -induced surface stress changes, but not their sign. Sample contraction (negative strain) as observed upon O_3-exposure in the present case (figure 2) requires generation of tensile surface stress (19). Qualitatively, such a behavior can be understood in terms of a strengthening of the in-plane metal-metal bonds e.g. by depopulation of antibonding metal states via charge transfer from the metal to the adsorbate.(*27*) For the Au/O system, the accumulation of negative charge on oxygen in the Au/O system is consistent with the higher Pauling electronegativity of O (3.44) with respect to Au (2.54), and has indeed been found in density functional theory (DFT) calculations (*28*). Note, however, that also the opposite effect has been observed. In electrochemical experiments, expansion of np-Au upon charge depletion in the surface layer was detected (*5*), in particular when the potential cycling includes strong OH adsorption/desorption. Such differences may be the result of deviating mechanisms with respect to the stress generation at metal-gas and metal-electrolyte interfaces. Whereas, charge-induced changes of the surface stress at solid-electrolyte interfaces seem to be dominated by classical electrostatic interaction of surface atoms with the surface excess charge,(*29*) adsorption on transition metal surfaces typically involves the formation of

localized (covalent) bonds whereby directly affecting the metal-metal bonding. Nevertheless, a relief of tensile surface stress upon oxygen adsorption from the gas phase cannot be generally excluded and has indeed been observed for the Pt(111)/O system.(*8*)

Beyond charge transfer, adsorbate-induced morphology changes may also play an important role, for example by changing the surface-to-volume ratio. Indeed, oxygen induced surface roughening via formation of Au-oxide nanoparticles has recently been observed in the Au(111)/O system (*30*). To be consistent with our observations, such morphology changes would be required to be reversible. For example, Au atoms released from Au-oxide particles by reaction with CO would be required to heal the defects created by the formation of these Au-oxide particles during O_3 exposure. In this context, the small irreversible strain component observed in our experiments might also be the result of irreversible morphology changes caused by oxygen-enhanced mass transport. Clearly, the origin of the oxygen-induced tensile surface stress generation observed in our experiments is not fully understood yet and will require more detailed studies.

Whether surface chemistry driven actuation will develop into an economically viable technology will strongly depend on materials costs, efficiency and long-term stability. The efficiency can be increased by using less energetic reactions than the oxidation of CO by O_3 used in the present work. This will require surface engineering to tailor the surface reactivity. Noble metal based systems such as np-Au can be replaced by lower-cost, lower-density, and stronger high surface area materials such as carbon aerogels, for example.

This work performed under the auspices of the U.S. Department of Energy by Lawrence Livermore National Laboratory under Contract DE-AC52-07NA27344.

1. R. H. Baughman, *Science* **308**, 63 (Apr, 2005).
2. V. H. Ebron *et al.*, *Science* **311**, 1580 (Mar, 2006).
3. J. Weissmueller *et al.*, *Science* **300**, 312 (Apr 11, 2003).
4. T. Mirfakhrai, J. D. W. Madden, R. H. Baughman, *Materials Today* **10**, 30 (Apr, 2007).
5. D. Kramer, R. N. Viswanath, J. Weissmuller, *Nano Lett.* **4**, 793 (May, 2004).
6. R. N. Viswanath, D. Kramer, J. Weissmuller, *Electrochimica Acta* **53**, 2757 (2008).
7. W. Haiss, *Reports on Progress in Physics* **64**, 591 (May, 2001).
8. H. Ibach, *Surface Science Reports* **29**, 193 (1997).
9. P. J. Feibelman, *Phys. Rev. B* **56**, 2175 (Jul, 1997).
10. N. Saliba, D. H. Parker, B. E. Koel, *Surface Science* **410**, 270 (Aug 1, 1998).
11. V. Zielasek *et al.*, *Angewandte Chemie-International Edition* **45**, 8241 (2006).
12. J. Erlebacher, M. J. Aziz, A. Karma, N. Dimitrov, K. Sieradzki, *Nature* **410**, 450 (2001).
13. J. Biener *et al.*, *Nano Lett.* **6**, 2379 (Oct 11, 2006).
14. J. A. van Bokhoven *et al.*, *Angewandte Chemie-International Edition* **45**, 4651 (2006).
15. R. C. Newman, S. G. Corcoran, J. Erlebacher, M. J. Aziz, K. Sieradzki, *MRS Bulletin* **24**, 24 (1999).
16. S. Cattarin, D. Kramer, A. Lui, M. M. Musiani, *Journal of Physical Chemistry C* **111**, 12643 (Aug, 2007).
17. J. Kim, E. Samano, B. E. Koel, *J. Phys. Chem. B* **110**, 17512 (Sep, 2006).
18. W. L. Yim *et al.*, *Journal of Physical Chemistry C* **111**, 445 (Jan, 2007).
19. The authors want to note that the ozone-induced sample contraction reported in this paper can only be observed if the sample has previously been exposed to CO to remove any surface oxide present. In contrast, ozone exposure of oxidized samples may result in sample expansion. In this case, continuous ozone exposure is required to maintain the sample strain, which is in contrast to the static nature of the surface stress induced effect discussed in this paper. In general, a sample expansion can be the result of sample heating via exothermic surface reactions. The authors also want to note that the role of residual Ag (1-7 at.%) in our np-Au samples is unclear and will be the subject of future studies.
20. A. M. Hodge *et al.*, *Acta Mater.* **55**, 1343 (Feb, 2007).
21. J. Kirn, E. Samano, B. E. Koel, *Surface Science* **600**, 4622 (Oct, 2006).
22. J. Weissmuller, J. W. Cahn, *Acta Mater.* **45**, 1899 (1997).
23. R. N. Viswanath, D. Kramer, J. Weissmuller, *Langmuir* **21**, 4604 (May, 2005).
24. H.-L. Duan, D. Farkas, S. G. Corcoran, J. Weissmüller, *in preparation*.
25. J. K. Diao, K. Gall, M. L. Dunn, *Journal of the Mechanics and Physics of Solids* **52**, 1935 (Sep, 2004).
26. M. Duchaineau, A. V. Hamza, T. Diaz De La Rubia, F. F. Abraham, *APL*, (submitted).
27. V. Fiorentini, M. Methfessel, M. Scheffler, *Phys. Rev. Lett.* **71**, 1051 (Aug, 1993).
28. D. Torres, K. M. Neyman, F. Illas, *Chemical Physics Letters* **429**, 86 (Sep, 2006).
29. Y. Umeno *et al.*, *Epl* **78**, (2007).

30. B. K. Min, A. R. Alemozafar, D. Pinnaduwage, X. Deng, C. M. Friend, *J. Phys. Chem. B* **110**, 19833 (Oct, 2006).
31. Part of this work was performed under the auspices of the U.S. Department of Energy by Lawrence Livermore National Laboratory under Contract DE-AC52-07NA27344. The authors want to express special thanks to Farid F. Abraham (LLNL) and Mark Duchaineau (LLNL) for generating the nanoporous Au samples for the MD simulations

Figure captions

Figure 1. Illustration of surface chemistry driven actuation in nanoporous gold. (**A**) Np-Au sample mounted in a viscous flow reactor (residence time ~ 1min). Adsorbate-induced dimensional changes of the np-Au sample are measured by dilatometry. (**B**) SEM micrograph showing the characteristic sponge-like open-cell morphology of np-Au. (**C**) Au surfaces can be switched back and forth between an oxygen-covered and clean state by alternating exposure to ozone (O_3) and carbon monoxide (CO). (**D**) Spring model illustrating the origin of adsorbate induced surface stress. Adsorbate-induced changes in the equilibrium distance a_o between surface atoms give rise to tensile ($a<a_o$) or compressive ($a>a_o$) surface stress.

Figure 2. Performance of a surface chemistry driven np-Au actuator. (**A**) Strain versus time as the np-Au actuator is alternately exposed to a mixture of ~7% O_3 in O_2 and pure CO. Between each exposure the sample compartment was purged for 3 min with ultrahigh purity N_2. Ozone exposure causes contraction, while CO exposure restores the original sample dimension. The response is mostly elastic, with only a small irreversible component. The system is very stable, and interrupting the exposure sequence for one hour causes only a small drift of the signal (**B**) Elastic strain amplitudes of up to 0.5% can be realized for long exposures. Note that a strain amplitude of 0.5 % corresponds to a macrocopic actuator stroke of 5 μm for a one-mm-long sample. The irreversible component becomes more pronounced for larger actuator strains. (**C**) Elastic strain versus ozone exposure time for a mixture of ~7% O_3 in O_2, and (**D**) elastic strain versus ozone concentration for 30 min exposures. Good reproducibility was obtained from different samples (■,▲). The actuator strain increases with both cycle length and O_3 concentration, and typical strain values lie in the range from 0.05 to 0.5%.

Figure 3: Surface stress induced relaxation of Au nanostructures studied by fully atomistic molecular dynamics (MD) simulations. (**A**) Nanoporous -Au and a (100) oriented Au nanowire resembling a ligaments of np-Au. Nanoporous Au foam samples were generated by simulating the spinodal decomposition during vapor quenching, and freezing the process once the desired length scale was achieved. (**B**) Surface stress induced relaxation of np-Au and Au nanowire samples during equilibration to zero overall pressure. In the case of nanowires, the effect of tensile surface stress is an almost uniaxial contraction along the wire axis ($\Delta L/L \sim \Delta V/V$) and the contraction is approximately seven times larger than predicted for a locally isotropic deformation (red line). Macroscopic isotropic contraction ($\Delta L/L \sim 1/3\ \Delta V/V$) is observed for np-Au consistent with the random network structure of this material.

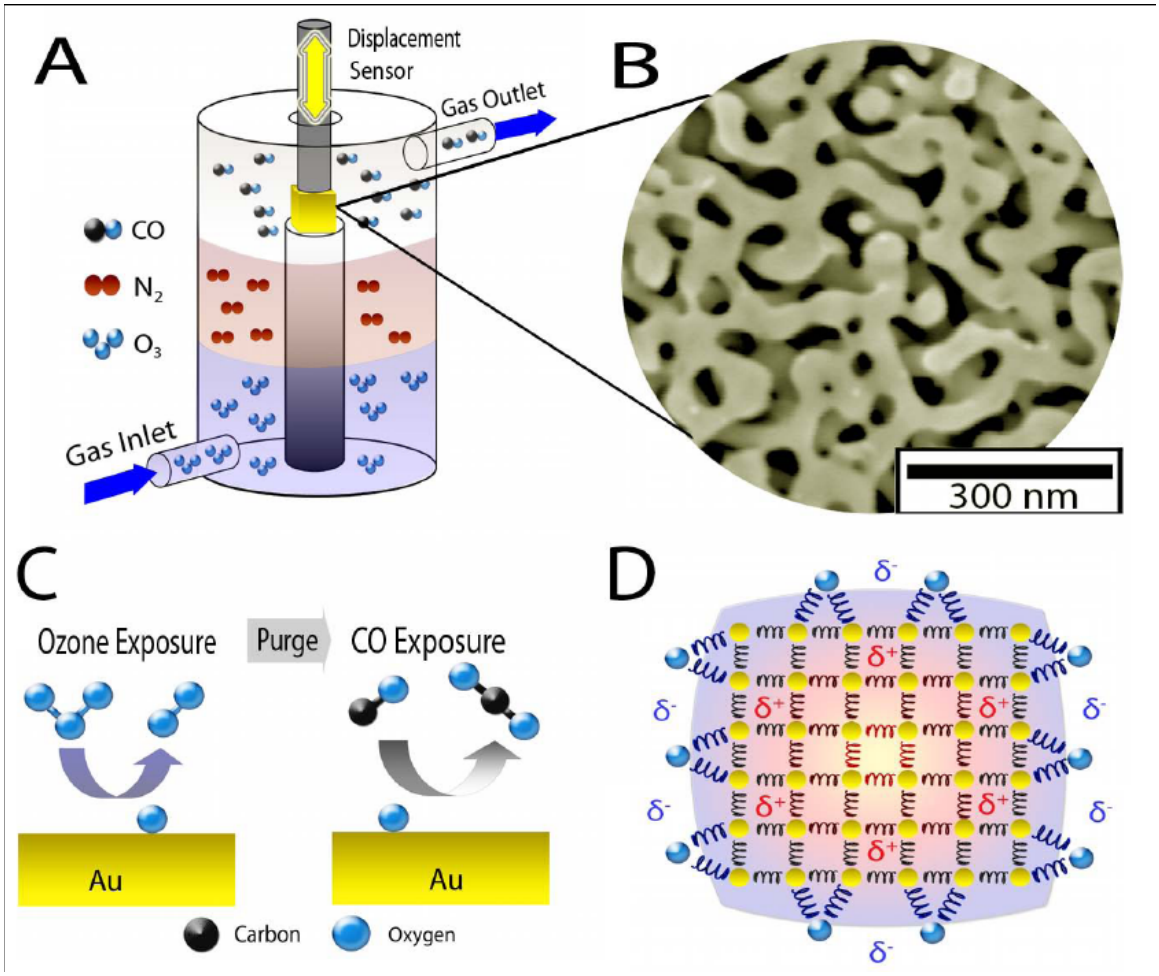

(A)

Figure 1. Illustration of surface chemistry driven actuation in nanoporous gold. (**A**) Np-Au sample mounted in a viscous flow reactor (residence time ~ 1min). Adsorbate-induced dimensional changes of the np-Au sample are measured by dilatometry. (**B**) SEM micrograph showing the characteristic sponge-like open-cell morphology of np-Au. (**C**) Au surfaces can be switched back and forth between an oxygen-covered and clean state by alternating exposure to ozone (O_3) and carbon monoxide (CO). (**D**) Spring model illustrating the origin of adsorbate induced surface stress. Adsorbate-induced changes in the equilibrium distance a_o between surface atoms give rise to tensile ($a<a_o$) or compressive ($a>a_o$) surface stress.

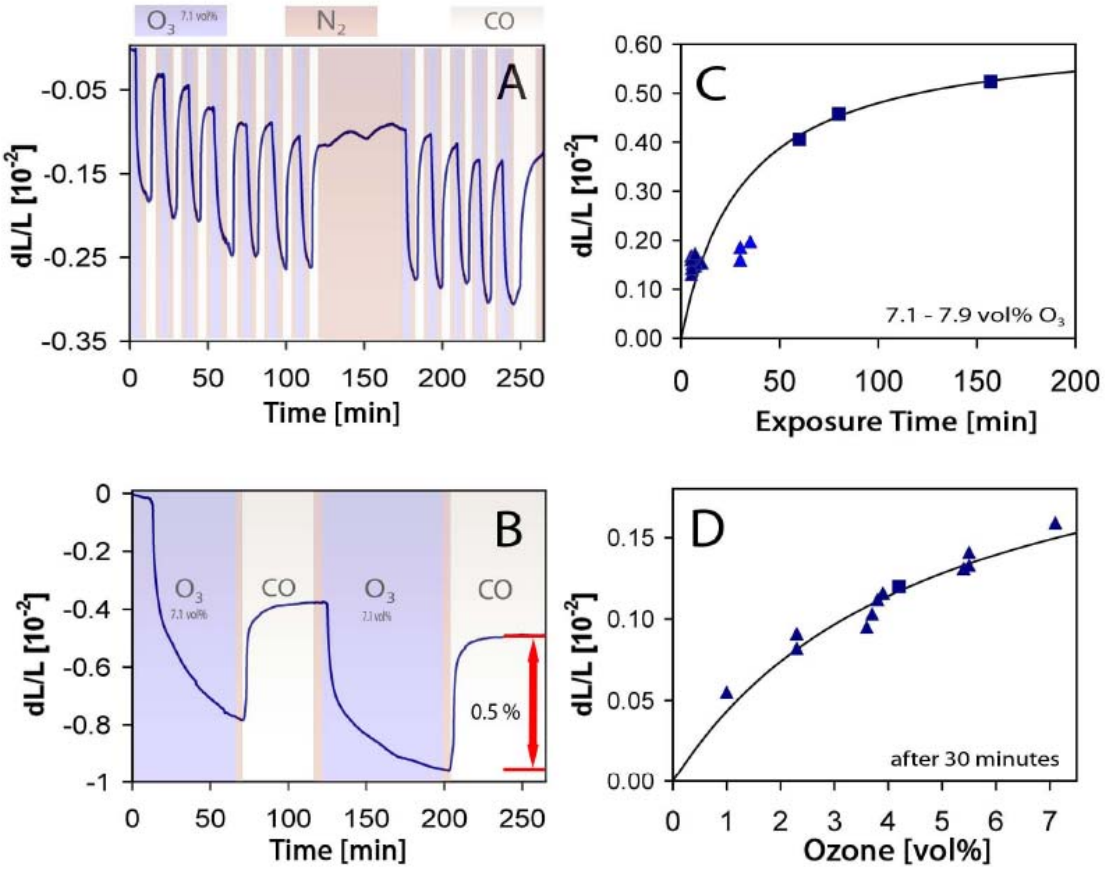

Figure 2. Performance of a surface chemistry driven np-Au actuator. (**A**) Strain versus time as the np-Au actuator is alternately exposed to a mixture of ~7% O_3 in O_2 and pure CO. Between each exposure the sample compartment was purged for 3 min with ultrahigh purity N_2. Ozone exposure causes contraction, while CO exposure restores the original sample dimension. The response is mostly elastic, with only a small irreversible component. The system is very stable, and interrupting the exposure sequence for one hour causes only a small drift of the signal (**B**) Elastic strain amplitudes of up to 0.5% can be realized for long exposures. Note that a strain amplitude of 0.5 % corresponds to a macroscopic actuator stroke of 5 μm for a one-mm-long sample. The irreversible component becomes more pronounced for larger actuator strains. (**C**) Elastic strain versus ozone exposure time for a mixture of ~7% O_3 in O_2, and (**D**) elastic strain versus ozone concentration for 30 min exposures. Good reproducibility was obtained from different samples (■,▲). The actuator strain increases with both cycle length and O_3 concentration, and typical strain values lie in the range from 0.05 to 0.5%.

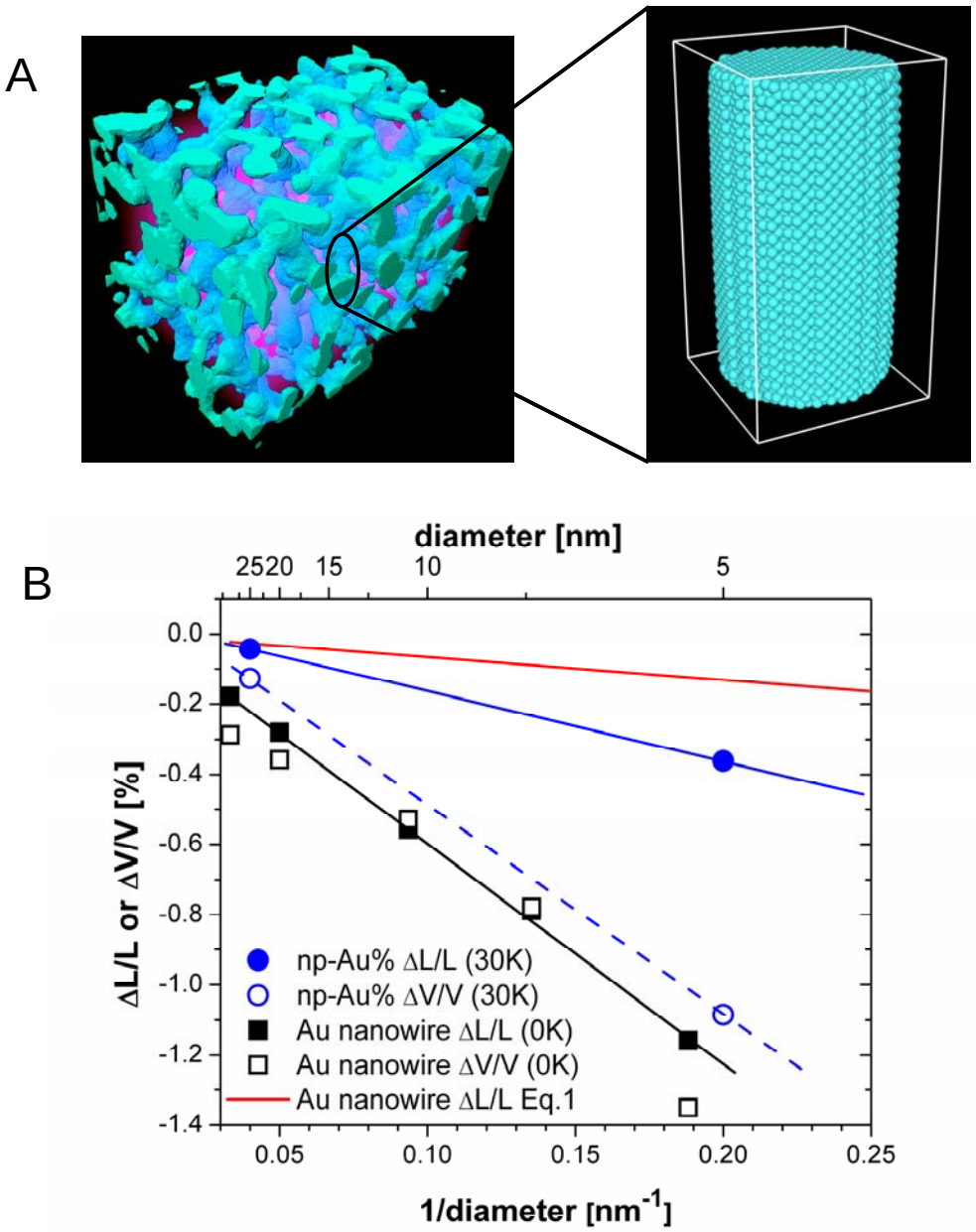

Figure 3: Surface stress induced relaxation of Au nanostructures studied by fully atomistic molecular dynamics (MD) simulations. (**A**) Nanoporous -Au and a (100) oriented Au nanowire resembling a ligaments of np-Au. Nanoporous Au foam samples were generated by simulating the spinodal decomposition during vapor quenching, and freezing the process once the desired length scale was achieved. (**B**) Surface stress induced relaxation of np-Au and Au nanowire samples during equilibration to zero overall pressure. In the case of nanowires, the effect of tensile surface stress is an almost uniaxial contraction along the wire axis ($\Delta L/L \sim \Delta V/V$) and the contraction is approximately seven times larger than predicted for a locally isotropic deformation (red line). Macroscopic isotropic contraction ($\Delta L/L \sim 1/3\ \Delta V/V$) is observed for np-Au consistent with the random network structure of this material.